A Volcano Rekindled: The Renewed Eruption of Mount St. Helens, 2004–2006
Edited by David R. Sherrod, William E. Scott, and Peter H. Stauffer
U.S. Geological Survey Professional Paper 1750, 2008

Chapter 29

Identification and Evolution of the Juvenile Component in 2004–2005 Mount St. Helens Ash

By Michael C. Rowe[1], Carl R. Thornber[2], and Adam J.R. Kent[3]

Abstract

Petrologic studies of volcanic ash are commonly used to identify juvenile volcanic material and observe changes in the composition and style of volcanic eruptions. During the 2004–5 eruption of Mount St. Helens, recognition of the juvenile component in ash produced by early phreatic explosions was complicated by the presence of a substantial proportion of 1980–86 lava-dome fragments and glassy tephra, in addition to older volcanic fragments possibly derived from crater debris. In this report, we correlate groundmass textures and compositions of glass, mafic phases, and feldspar from 2004–5 ash in an attempt to identify juvenile material in early phreatic explosions and to distinguish among the various processes that generate and distribute ash. We conclude that clean glass in the ash is derived mostly from nonjuvenile sources and is not particularly useful for identifying the proportion of juvenile material in ash samples. High Li contents (>30 µg/g) in feldspars provide a useful tracer for juvenile material and suggest an increase in the proportion of the juvenile component between October 1 and October 4, 2004, before the emergence of hot dacite on the surface of the crater on October 11, 2004. The presence of Li-rich feldspar out of equilibrium (based on Li-plagioclase/melt partitioning) with groundmass and bulk dacite early in the eruption also suggests vapor enrichment in the initially erupted dacite. If an excess vapor phase was, indeed, present, it may have provided a catalyst to initiate the eruption. Textural and compositional comparisons between dome fault gouge and the ash produced by rockfalls, rock avalanches, and vent explosions indicate that the fault gouge is a likely source of ash particles for both types of events. Comparison of the ash from vent explosions and rockfalls suggests that the fault gouge and new dome were initially heterogeneous, containing a mixture of conduit and crater debris and juvenile material, but became increasingly homogeneous, dominated by juvenile material, by early January 2005.

Introduction

The phreatic explosion at Mount St. Helens, Wash., on October 1, 2004, was the first of four such events that occurred between October 1 and 5, 2004, preceding the emergence of hot dacitic lava on the crater floor on October 11, 2004. From October 5, 2004, through December 2005, two additional explosions and numerous rockfalls sent volcanic ash over the crater rim (Scott and others, this volume, chap. 1).

Petrologic characterization of volcanic ash provides a means to monitor volcanic activity and to assess precursory evidence of changes in eruptive behavior (Taddeucci and others, 2002). Volcanic monitoring by way of ash characterization is commonly conducted because ash may be collected easily at relatively low cost. Also, because the volcanic edifice is not always accessible, volcanic ash may provide the only petrologic evidence for changes in eruptive behavior.

Juvenile magmatic glass has been observed in the tephra produced before extrusion of lava flows and domes or before large magmatic eruptions (Watanabe and others, 1999; Cashman and Hoblitt, 2004). "Juvenile," as defined in this study, refers to ash and dome lava erupted hot, with textural and geochemical characteristics similar to the earliest dome material (sample SH304, collected Nov. 4, 2004) and later dome samples. (Dome samples dredged from the crater floor before sample SH304 was collected consist of a heterogeneous mixture of crater and conduit debris and minor juvenile material; Pallister and others, this volume, chap. 30). Monitor-

[1] Department of Geosciences, 104 Wilkinson Hall, Oregon State University, Corvallis, OR 97331; now at Department of Geoscience, 121 Trowbridge Hall, University of Iowa, Iowa City, IA 52242

[2] U.S. Geological Survey, 1300 SE Cardinal Court, Vancouver, WA 98683

[3] Department of Geosciences, 104 Wilkinson Hall, Oregon State University, Corvallis, OR 97331

ing of glass compositions in volcanic ash has also identified multiple magmatic components in eruptions and recorded compositional change over the course of a single eruption (for example, Pallister and others, 1992; Swanson and others, 1994, 1995; Schiavi and others, 2006).

At Mount St. Helens, previous eruptive products complicate the ash story, making petrologic monitoring of volcanic ash more difficult. Lava-dome growth from 1980 to 1986 generated a thick (~250 m) cap of dacitic lava over the preexisting conduit. In addition, crater-filling breccia and tephra from 1980 and earlier eruptions may underlie the 1980–86 lava dome for 500 m or more (Friedman and others, 1981). Ash produced by explosions is therefore likely to contain a substantial proportion of "older" Mount St. Helens material. Analysis and comparison of ash is further complicated by mechanical sorting during transport, requiring consideration of such variables as sample location relative to the vent and windspeed and wind direction (for example, Sparks and others, 1997; Houghton and others, 2000).

Petrologic studies of older Mount St. Helens tephra provide a basis for comparing the products of the 2004 eruption (ongoing at time of writing, early 2007). Glass analyses of 1980–82 tephra and dome samples demonstrated trends of increasing crystallinity and decreasing water content, with lower water content likely associated with progressively lower volume and less intense post-May 18 explosive eruptions (Sarna-Wojcicki and others, 1981a; Melson, 1983). Textural comparisons of the May 18, 1980, blast material with that from precursory eruptions indicate that juvenile material appeared as early as 2 months before the climactic eruption and that the juvenile component was reflected by ash particles with either glassy or microcrystalline matrices, characteristic of shallow crystallization (Cashman and Hoblitt, 2004). Cashman and Hoblitt's study is significant in that it identifies the need to consider partially crystalline material in addition to glassy fragments as potentially juvenile. Also, it provides a textural comparison for current eruptive products.

Several previous studies of trace elements, capable of transport within volatile phases, in tephras were undertaken to identify evidence for magmatic degassing associated with explosive events before and after May 18, 1980 (Thomas and others, 1982; Berlo and others, 2004). Whole-rock ^{210}Pb excess and Li enrichment (max ~23 µg/g) in plagioclase feldspar in the 1980 cryptodome, followed by significantly lower Li contents in feldspar within the May 18 fallout tephra and pyroclastic-flow deposits and subsequent eruptive events, led Berlo and others (2004) to propose that the anomalously high Li contents resulted from vapor transfer from a deeper magma source to shallow stored/stalled magma.

The goals of this study of 2004–5 Mount St. Helens ash were to (1) identify and track changes over time in the composition and proportion of juvenile eruptive material in explosive events associated with the reactivation of Mount St. Helens; and (2) combine textural and geochemical observations to distinguish between the processes and products of ash generation, including a comparison of ash from rockfalls and vent explosions. Accomplishing these goals required a detailed examination of the textures and geochemical characteristics of erupted ash samples in comparison with dome petrology and geochemistry, discussed elsewhere in this volume (Cashman and others, this volume, chap. 19; Pallister and others, this volume, chap. 30; Thornber and others, this volume, chap. 32; Kent and others, this volume, chap. 35).

Methods

Sample Collection

After the October 1, 2004, phreatic eruption of Mount St. Helens, 27 ash-collection stations were established around the perimeter of the volcano (fig. 1). Ash samples collected before the placement of stations were from relatively clean flat surfaces (fig. 2*A*). Collection stations were distributed radially along line-of-sight to the volcano, ranging in distance from 2.4 to 10 km from the vent (fig. 1). Each station consisted of a rebar-suspended double bucket (fig. 2*B*); the inner bucket, with drainage slits approximately a third up from its base, was suspended within the outer bucket to allow excess water to drain without significant loss of ash. Ash was collected at stations over periods ranging in length from less than 3 to more than 15 days until November 29, 2004 (fig. 3). Ultimately, ash collection at the established stations was a function of station accessibility, whereas the presence of ash depended on predominant wind directions during the period preceding

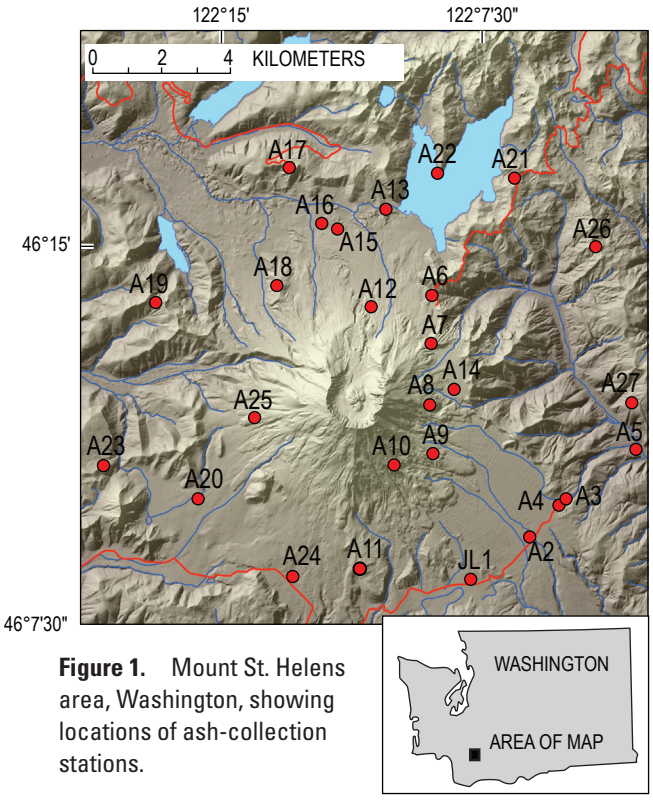

Figure 1. Mount St. Helens area, Washington, showing locations of ash-collection stations.

collection. After November 29, 2004, most ash samples were collected from discrete ash-producing events (either explosions or rockfalls and rock avalanches) on snow-covered (fig. 2*C*) or otherwise-clean surfaces. Snow-covered surfaces provided easy identification of new ash and allowed for tracking of deposited ash to its source (fig. 2*C*). Additional ash samples were collected in August 2005 from collection devices placed in the crater ("petrology spiders," fig. 2*D*), similar to those deployed for seismic and deformation monitoring (LaHusen and others, this volume, chap. 16).

A total of 15 samples collected between October 1, 2004, and March 9, 2005, were analyzed in this study (table 1), of which 12 are of ash spanning the period October 1, 2004, through March 9, 2005, two are of dome fault gouge (collected Nov. 4, 2004, and Feb. 22, 2005), and one is from a crater debris flow (collected Oct. 20, 2004) associated with collapse of the initial spine (table 1). (See Pallister and others this volume, chap. 30, for a detailed description of dome fault gouge and crater debris flow collection.)

Of the four early explosive events, only the three included in this study (12:02 p.m. Oct. 1, 9:43 a.m. Oct. 4, and 9:05 a.m. Oct. 5) produced downwind ash fallout between October 1 and October 5, 2004 (Major and others, 2005). Samples from the suite of Mount St. Helens 2004–5 ash deposits (Rowe and others, 2008) were selected for our purposes on the basis of emplacement date, wind directions, and volume of material collected.

Analytical Methods

Major-element compositions of groundmass glass, melt inclusions (where possible), feldspar, and mafic minerals (amphibole, clinopyroxene, and hypersthene) were measured

Figure 2. Examples of ash-collection sites. *A*, Clean, flat surfaces. *B*, At an ash collection station. Inset is a schematic drawing of the ash-collection buckets, showing drainage slits in upper bucket and drainage holes in base of lower bucket; bolts in lower bucket provide support and suspension of upper bucket. *C*, On snow-covered surfaces. *D*, In petrology spiders (see text for description). Inset is top view of petrology spider, with nylon netting for identification and collection of hot ballistic material on left and baffled compartments for ash and lithic fragments on right.

Table 1. Ash, gouge, and crater debris samples analyzed in this study.

[Eruption dates for crater debris and gouge samples estimated by J.S. Pallister. Further details of ash samples are available in Rowe and others (2008).]

Sample	Type	Date collected	Eruption date
MSH04E1DZ_1	ash	10/1/2004	10/1/2004
MSH04E2A03_A1	ash	10/4/2004	10/4/2004
MSH04E3RANDLE_2	ash	10/5/2004	10/5/2004
MSH04A20_10_11	ash	10/11/2004	10/5/04–10/11/04
MSH04A09_10_12	ash	10/12/2004	10/4/04–10/12/04
MSH04A20_10_16	ash	10/16/2004	10/11/04–10/16/04
MSH04A21_10_20	ash	10/20/2004	10/15/04–10/20/04
MSH04A04_11_2	ash	11/2/2004	10/16/04–11/2/04
MSH04MR_11_4	ash	11/4/2004	11/4/2004
MSH05JP_1_14A	ash	1/14/2005	1/13/2005
MSH05JV_1_19	ash	1/19/2005	1/16/2005
MSH05DRS_3_9_4	ash	3/9/2005	3/8/2005
SH303-1	gouge	11/4/2004	10/18/04
SH307-1	gouge	2/22/2005	2/12/05
SH300-1	crater debris[1]	10/20/2004	10/15/04

[1]Only fine material collected from the crater debris flow is included in this study; includes 2004 dacite as well as older crater-floor debris.

for all 12 ash samples by electron microprobe analysis. To reduce potential sampling biases, 25 to 50 feldspar phenocrysts, ~20 mafic phenocrysts, and 10 to 20 glass specimens were analyzed from each sample, approximately proportional to their relative abundances in ash samples, as estimated visually. Backscattered electron images were taken of all the ash and dome gouge samples to document the heterogeneity of ash particles within and between samples. Trace-element contents in feldspar from 14 samples were measured by laser-ablation inductively coupled plasma mass spectrometry (LA-ICP-MS). In addition, major- and trace-element contents in feldspar from the two dome fault-gouge samples (SH303-1 and SH307-1, table 1) and trace-element contents in feldspar from the crater debris sample (sample SH300-1, table 1) were determined.

Electron microprobe analyses were conducted on a Cameca SX–100 instrument at Oregon State University. Analyzed samples were not sieved, and phenocrysts and glasses of all sizes were analyzed to reduce the possible bias created by mechanical sorting during transport (Houghton and others, 2000). Wherever possible, electron microprobe analyses of phenocryst phases were made within 15 µm of the grain boundary. Electron microprobe analyses of glass were conducted according a procedure modified from that of Morgan and London (1996). Na and K were counted for 60 s, using a 2-nA beam current, a 15-keV accelerating voltage, and a 10-µm beam diameter. Al, Ca, Cl, Fe, Mg, Mn, P, S, Si, and Ti were analyzed by using a 30-nA beam current, a 15-keV accelerating voltage, and 10-µm beam diameter, with count times ranging from 10 to 50 s. The narrow beam diameter (~20 µm is optimal) was required by the small size of glassy fragments in the ash (Morgan and London, 1996). Feldspar (30 nA) and mafic phases (50 nA) were measured by using a 15-keV accelerating voltage and 5- and 1-µm beam diameters, respectively. A rhyolite glass standard (USNM 72854 VG–568), a feldspar standard (Labradorite USNM 115900), and a pyroxene standard (Kakanui augite USNM 122142) were analyzed before each analytical session. Glass standard statistics are presented in Rowe and others (2008).

Trace-element (Ba, Ce, Eu, La, Li, Nd, Pb, Pr, Sr, and Ti) contents in feldspar were determined by LA-ICP-MS analysis in the W.M. Keck Collaboratory for Plasma Spectrometry at Oregon State University, using a 193-nm ArF Excimer laser. Analyses were performed by using a stationary laser (70-µm spot size) to ablate a progressively deepening crater in the sample materials, requiring targeted feldspar phenocrysts to be larger than ~80 µm in diameter. Owing to the large spot size required and the fine grain size of the feldspar in the ash, analyses were made close to the center of inclusion-free grains. Each individual analysis represents 40 s of data acquisition during ablation, with background

count rates measured for 30 s before ablation. A 4-Hz pulse frequency resulted in an ablation crater 15 to 20 μm deep. Trace-element abundances were calculated relative to the NIST 612 glass standard, which was analyzed under identical conditions throughout the analytical session. U.S. Geological Survey glass BCR-2G was also analyzed as a secondary standard. Counts were normalized to ^{29}Si, also measured during ablation, and contents were determined according to the method of Kent and others (this volume, chap. 35). Precision of trace-element analysis is presented by Kent and others (this volume, chap. 35). Li contents, most relevant to this study, have a precision of 7 to 8 percent (1σ), although for one session, involving measurement of samples SH300-1, MSH04A20_10_16, and MSH05DRS_3_9_4 (table 1), analytical uncertainties calculated from repeated analyses of standard BCR-2G may be as high as 25 percent (1σ). Overall, uncertainties are similar to those in the analyses by Berlo and others (2004) and Kent and others (this volume, chap. 35), who reported analytical uncertainties of ~10–15 percent.

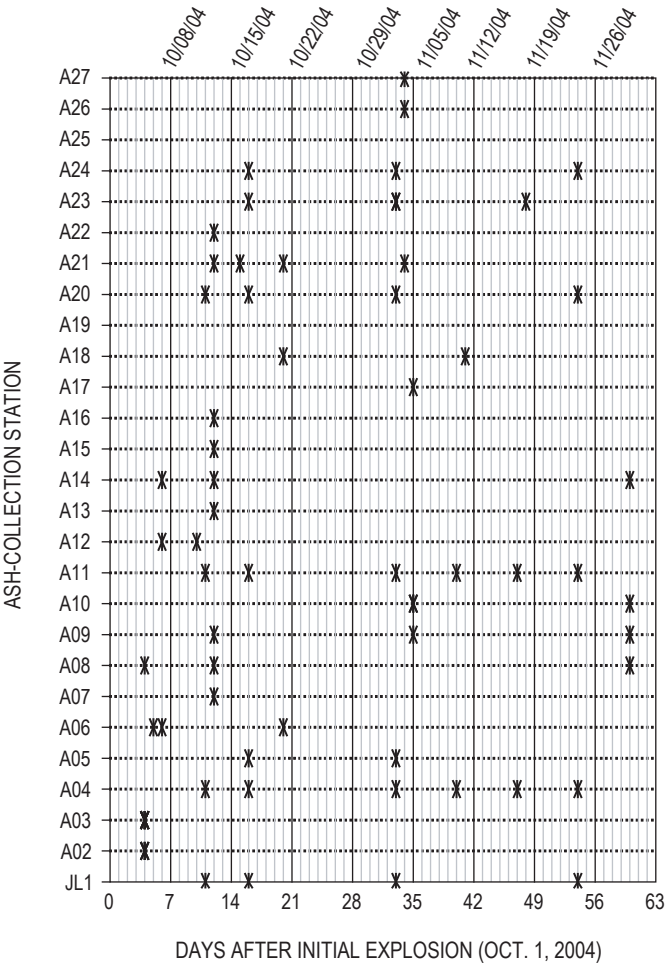

Figure 3. Collection dates for ash-collection stations (see fig. 1) from October 1 (day 0) through November 29 (day 60), 2004.

Results

Glass and Groundmass

The groundmass in ash samples is dominated by crystalline to microcrystalline textures, with groundmass crystallization resulting in the formation of crystalline silica and feldspar microlites (fig. 4). Matrix textures of the juvenile dacite are described elsewhere in this volume (Cashman and others, this volume, chap. 19; Pallister and others, this volume, chap. 30). Late crystallization of the groundmass significantly influenced glass analyses. Al_2O_3 and SiO_2 contents were used to screen glass analyses for microlite crystallization (fig. 4), resulting in 81 reliable analyses of glass, herein referred to as "clean glass." Most clean-glass analyses were obtained from pumice fragments and glass adhering to phenocrysts. Major-element contents in clean glass vary widely, likely owing to localized effects of melt crystallization and the inherent heterogeneity of the ash, especially in early explosions. SiO_2 contents in clean glass range from 52 to 79 weight percent but dominantly are from 72 to 78 percent (table 2). No temporal trend is apparent to suggest a systematic change in the melt composition over the course of 2004–5 sampling (fig. 5).

Mafic Minerals

Mafic minerals analyzed in the ash samples include hypersthene, amphibole, clinopyroxene, and olivine. Hypersthene, which is the dominant mafic mineral in the ash, varies widely in composition ($En_{47.1–73.7}$). Hypersthene in dome sample SH304-2 ($En_{53.3–65.8}$), as well as in older 1980s dome samples ($En_{44.3–69.8}$), similarly varies widely in composition (fig. 6). Amphibole compositions in the ash, new dome dacite, and the 1980–86 dome dacite are essentially identical, most easily observed in Al_2O_3 and FeO* contents. Al_2O_3 content ranges from ~7 to 14 weight percent in the ash and 1980–86 dome material and from ~6 to 15 weight percent in the 2004–6 dome dacite, although in all three samples Al_2O_3 contents cluster between 10 and 13 weight percent (fig. 7). Similarly, total Fe contents range from ~10 to 18 weight percent FeO* in the ash, 1980–86 dome, and 2004–6 dome (fig. 7; Rutherford and Devine, this volume, chap. 31; Thornber and others, this volume, chap. 32).

The thickness of the outermost disequilibrium-reaction rims on amphibole phenocrysts in the ash varies widely, with thick reaction rims (>15–20 μm) present on some grains. Disequilibrium-reaction rims on amphiboles from new dome dacite typically are ~5 μm thick, sporadically 6 to 10 μm thick, and rarely 50 to 100 μm thick, with larger rims commonly associated with amphibole xenocrysts (Thornber and others, this volume, chap. 32). Variations in thickness of amphibole disequilibrium-reaction rims decreased over the course of the eruption, with only rare thick rims in March 8, 2005, tephra. The presence of thick-rimmed amphibole grains is characteristic of 1980–86 magmas (Rutherford and Hill, 1993) but differs from the uni-

Table 2. Electron microprobe analyses of clean, juvenile glass.

[Juvenile glass as described in text is based on MgO and K_2O fields defined by glass and inclusion analyses of samples SH304 and SH305. Specific analysis from among a suite is listed in "Analysis" column. Total Fe reported as FeO. nd, not determined. Sample prefixes MSH04 and MSH05 have been removed; see table 1 for complete sample numbers.]

Sample	Analysis	SiO_2	TiO_2	Al_2O_3	FeO	MnO	MgO	CaO	Na_2O	K_2O	P_2O_5	SO_2	Cl	Total
E2A03_A1	2	73.30	0.47	14.72	1.19	0.05	0.22	1.40	4.37	2.75	0.09	0.01	0.14	98.71
E2A03_A1	7	74.00	0.27	15.91	0.89	0.00	0.06	2.09	4.28	2.83	0.07	0.00	0.04	100.44
A20_10_11	11	72.32	0.26	15.02	1.21	0.04	0.09	1.66	4.77	2.28	0.08	0.01	0.12	97.86
A20_10_16	2	76.81	0.24	13.79	1.42	0.02	0.16	0.52	2.92	4.52	0.04	0.00	0.09	100.53
A20_10_16	4	77.63	0.34	12.64	0.97	0.00	0.05	0.57	3.15	4.21	0.03	0.00	0.02	99.61
A21_10_20	14	74.75	0.34	14.24	0.53	0.00	0.02	1.24	3.97	3.41	0.07	0.01	0.01	98.59
A04_11_2	16	71.52	0.22	18.38	0.97	0.00	0.06	2.70	4.26	3.28	0.06	0.00	0.00	101.45
JP_1_14A	1	75.49	0.22	14.00	0.47	0.00	0.10	1.00	4.47	4.12	0.05	0.01	0.05	99.98
JP_1_14A	2	76.06	0.23	12.60	1.32	0.00	0.00	0.33	5.49	3.19	0.18	0.01	0.05	99.46
JP_1_14A	3	73.83	0.18	15.34	0.63	0.02	0.04	1.70	4.45	4.49	0.03	0.01	0.01	100.73
JP_1_14A	6	76.01	0.22	13.78	0.53	0.00	0.09	1.22	2.77	5.33	0.23	0.01	0.03	100.22
JP_1_14A	9	78.38	0.16	12.69	0.64	0.01	0.03	1.29	1.62	5.01	0.04	0.00	0.03	99.90
JV_1_19	4	74.14	0.26	16.05	1.44	0.05	0.07	1.50	5.54	3.03	0.09	0.00	0.02	102.19
JV_1_19	8	71.17	0.09	16.05	0.42	0.01	0.03	1.68	4.55	2.28	0.05	0.02	0.03	96.38
SH304-2 [1]	A9b hb1	75.2	0.19	13.5	0.87	0.00	0.01	0.88	2.32	5.09	0.01	nd	0.103	98.27
SH305-1 [1]	kc g-22	76.6	0.34	12.4	1.35	0.01	0.03	0.27	3.01	5.72	0.08	nd	0.110	99.92

[1]Representative analyses of dome samples SH304 and SH305 from Pallister and others (this volume, chap. 30).

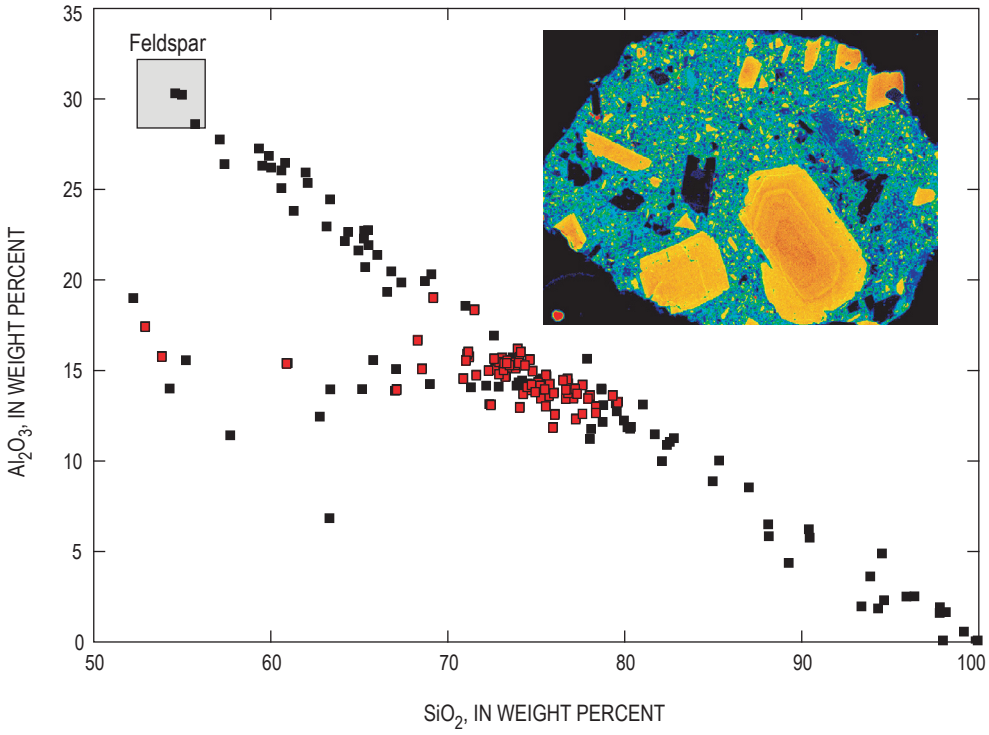

Figure 4. Silica-variation diagram showing Al_2O_3 versus SiO_2 contents in groundmass glass of ash fragments. Compositional range between feldspar and quartz end members is characteristic of highly crystalline groundmass. Red data points, clean glass (see text for explanation). Inset X-ray map (Al Kα) shows crystallization of feldspar (orange) and quartz (blue) in juvenile groundmass.

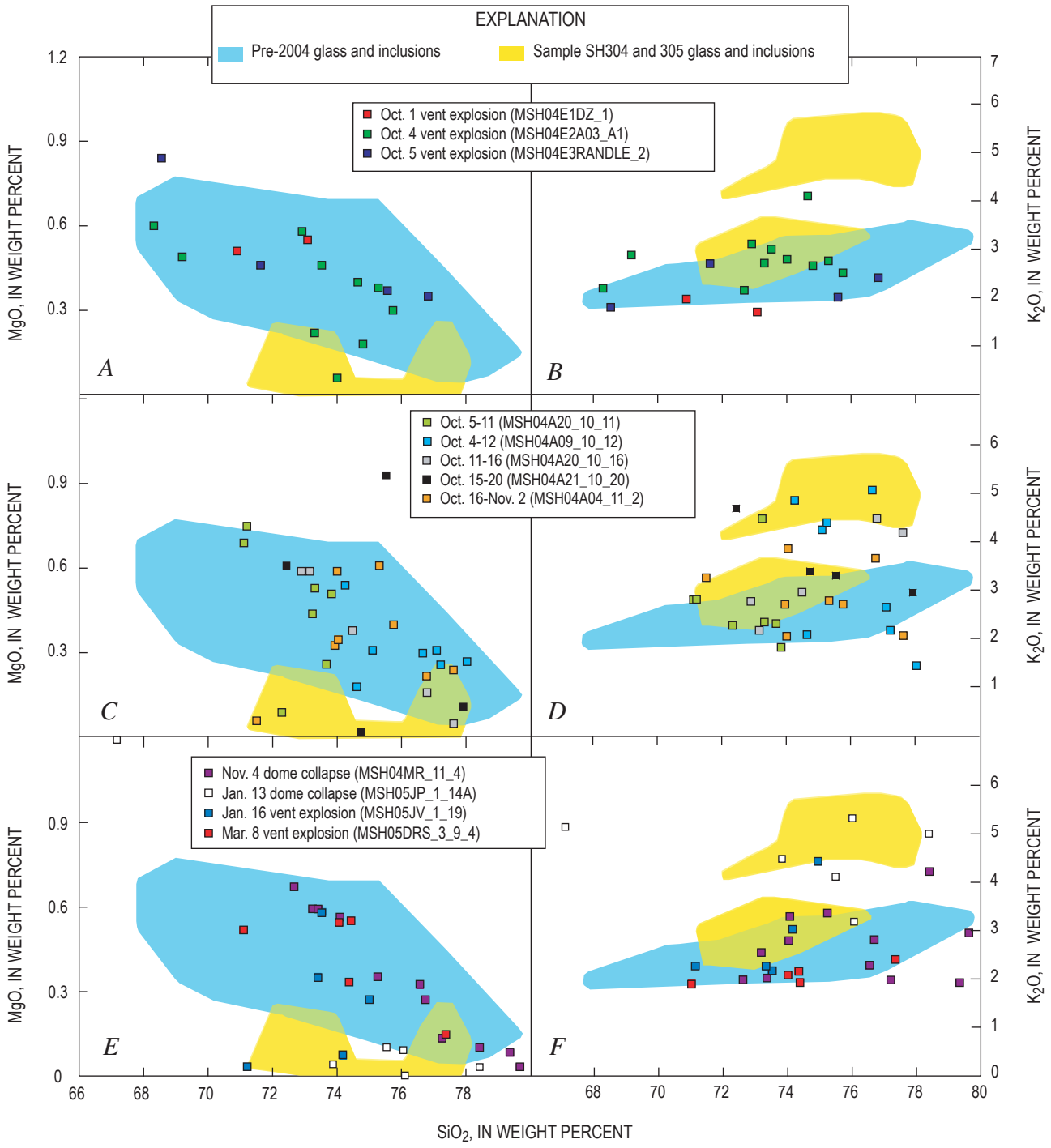

Figure 5. Silica-variation diagrams of MgO and K_2O versus SiO_2 contents in clean glass (see text for explanation). Blue field, pre-2004 tephra and dome glass compositions (Sarna-Wojcicki and others, 1981a; Melson, 1983); yellow field, glass and melt-inclusion compositions for dome samples SH304 and SH305 from current explosions (see Pallister and others, this volume, chap. 30). Plots are paired to show tephra from early vent explosions *(A, B)*, tephra from October 5 to November 2, 2005 *(C, D)*, and tephra from rockfalls and vent explosions from November 4, 2004, to March 8, 2005 *(E, F)*.

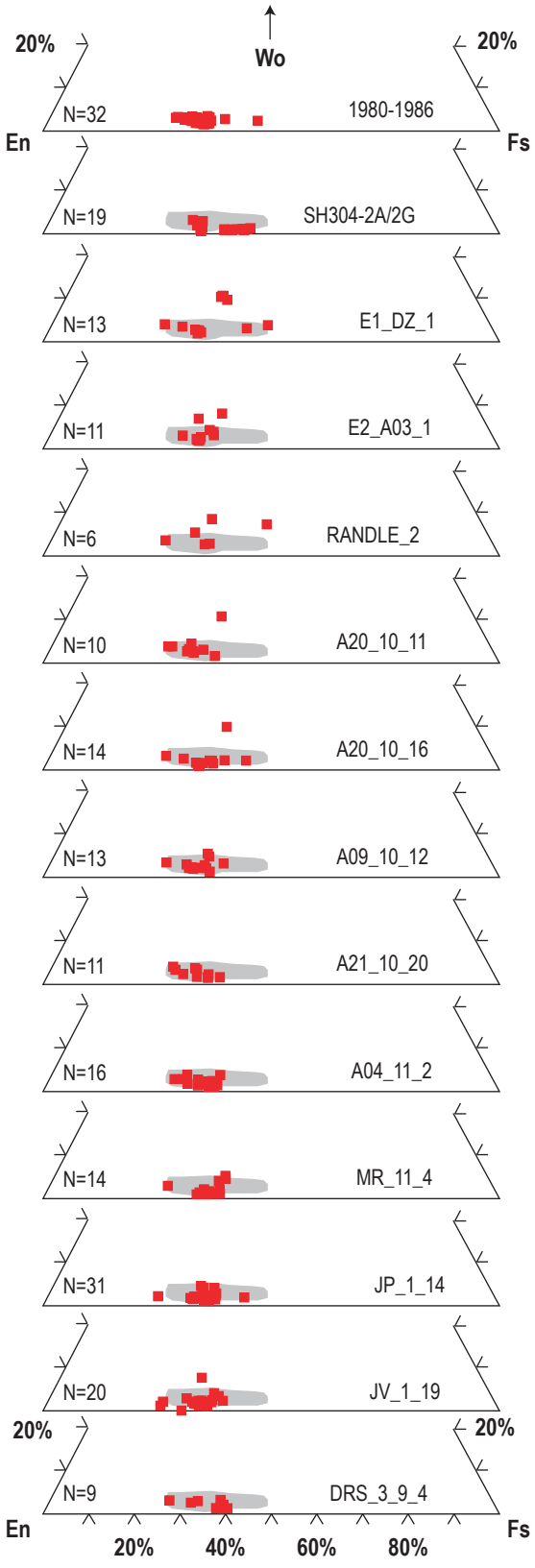

Figure 6. Compositions of hypersthene phenocrysts analyzed from 1980–86 Mount St. Helens, dome sample SH304-2A, and 2004–5 ash samples. Shaded field, range of 1980–86 hypersthene compositions from top panel.

formly thin (~5 µm thick) decompression rim around 2004–5 dacitic amphiboles, an observation suggesting that the early ash samples have older Mount St. Helens material mixed with juvenile ash particles.

In addition to the presence of thick reaction rims on amphibole phenocrysts in the ash, the identification of clinopyroxene and rare olivine phenocrysts in the early ash supports the interpretation that these samples were a heterogeneous mixture containing some proportion of older Mount St. Helens eruptive material. Discrete clinopyroxene phenocrysts are present in the early ash samples but rare in the new dome material, where they typically are associated with xenolith fragments. Clinopyroxene phenocrysts were not observed in the ash samples collected after October 20, 2004.

Owing to the compositional variation of hypersthene and amphibole phenocrysts in the ash samples and the complete compositional overlap between these phases in the new dome and 1980–86 dome, mafic-mineral phases are of limited value for identification of juvenile material and are not discussed further here. (See Rutherford and Devine, this volume, chap. 31, and Thornber and others this volume, chap. 32, for discussion of the textural and compositional variations of Mount St. Helens 2004–5 amphiboles.)

Feldspars

Feldspar phenocrysts in ash, gouge, and crater debris vary widely in composition. Feldspar phenocryst compositions in the ash range from An_{87} to An_{28}, overlapping samples from both the new dome ($An_{53–33}$) and 1980–85 dome ($An_{51–34}$). As with mafic-mineral phases, major-element contents in feldspar

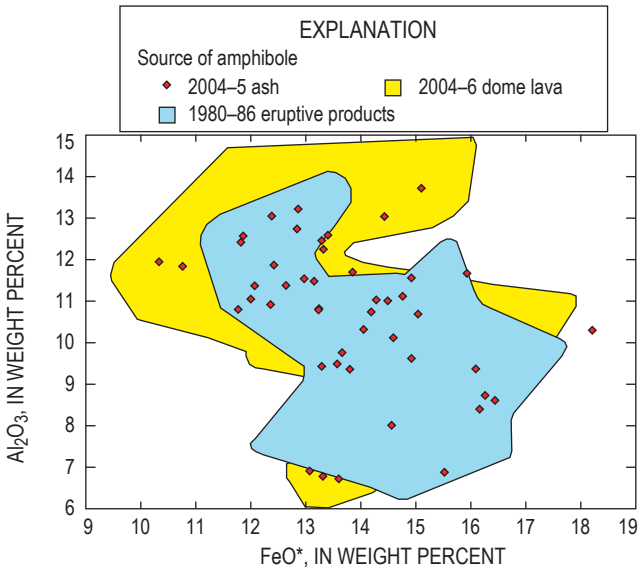

Figure 7. Al_2O_3 versus total Fe (FeO*) in amphiboles in ash samples. Blue field, amphibole in 1980–86 eruptive material; yellow field, amphibole in 2004–6 dome material.

in the ash and new dome samples are indistinguishable from older Mount St. Helens eruptive material (Rowe and others, 2005; Streck and others, this volume, chap. 34). A total of 266 LA-ICP-MS analyses were completed on 14 of the samples included in this study. Significant variations were noted in the contents of Ba (14.5–224 µg/g), Sr (532–1,603 µg/g), La (1.0–9.7 µg/g), Pb (0.3–7.0 µg/g), and Li (6.9–48.5 µg/g) (Rowe and others, 2008). La has a well-defined, and Pb a weakly defined, positive correlation with Ba, whereas Sr is negatively correlated with Ba (fig. 8). Correlations between trace elements (excluding Li) and anorthite content are believed to be due both to variations in feldspar/melt partition coefficients with anorthite content and to changes in melt composition as a result of fractionation of plagioclase, hornblende, hypersthene, and oxides during melt evolution (Kent and others, this volume, chap. 35).

Li in feldspar, in contrast to other trace elements, does not correlate with other major or trace elements. In addition, on the basis of feldspar/melt partitioning, the highest Li contents would require >>200 µg/g Li in the melt (Bindeman and others, 1998), significantly greater than that observed in the bulk dacite (21–28 µg/g; Kent and others, 2007; Thornber and others, 2008b). In ash samples collected after November 4, 2004, Li contents are more homogenous and consistently lower relative to earlier ash samples, with a maximum Li content of 30 µg/g (fig. 9). This decrease in Li content was also observed in dome samples collected after Mount St. Helens dome sample SH304, which was estimated to have been erupted on or about October 18, 2004 (Kent and others, 2007; Pallister and others, this volume, chap. 30; Kent and others, this volume, chap. 35).

Discussion

October 1–5, 2004, Ash Explosions

Identification of a Juvenile Component

Identification and quantification of the juvenile component in the products of early Mount St. Helens eruptive events can be used to evaluate the likely course of a reawakening volcano. By comparing glass compositions and feldspar trace-element contents in the ash with those of 1980–86 and 2004–5 dome materials, the proportion of juvenile material (if present), as previously defined, in the early erupted ash may be

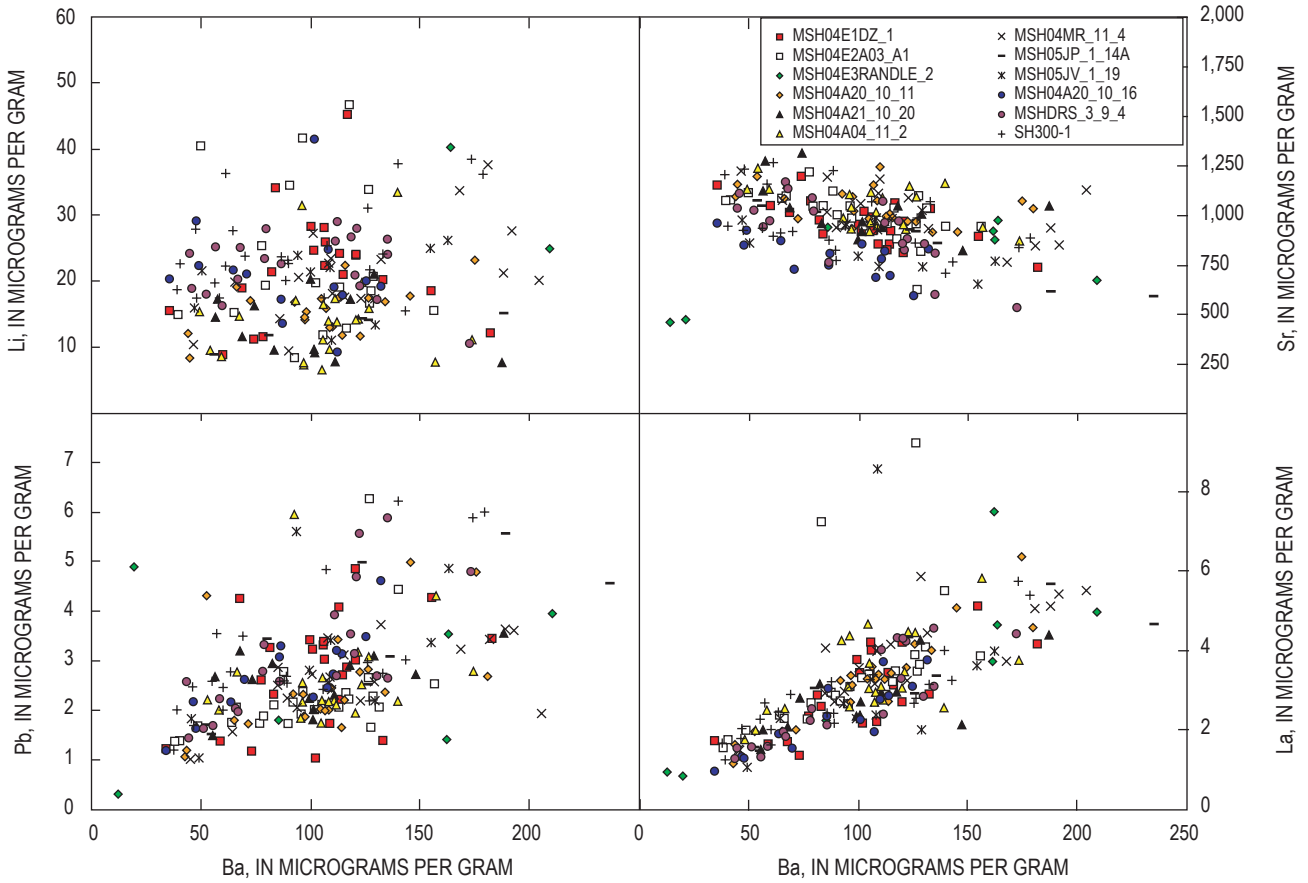

Figure 8. Selected trace-element contents in feldspar in ash samples.

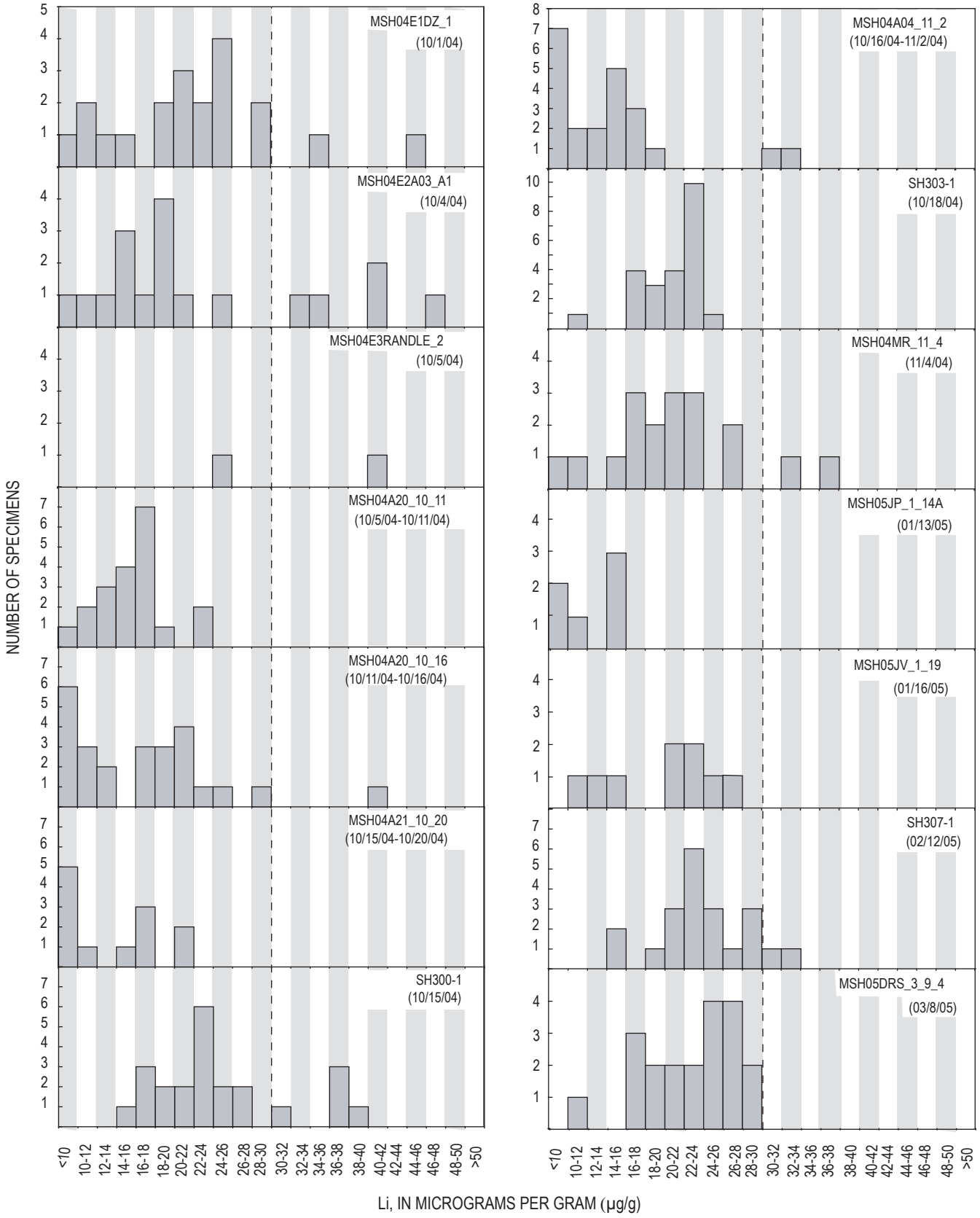

Figure 9. Histograms of Li contents in feldspar from each of 14 analyzed samples. Feldspar Li contents >30 µg/g (dashed line) in ash samples collected before November 4, 2004, coincide with Li contents in juvenile feldspar from dome sample SH304. Eruption dates of samples are given in parentheses.

calculable. Most major-element contents in glass overlap with those in eruptive products of 1980–82 (Sarna-Wojcicki and others, 1981a; Melson, 1983) and pre-1980 (Sarna-Wojcicki and others, 1981a). However, matrix glass and melt inclusions from 2004–5 Mount St. Helens samples SH304 and SH305 have distinctly lower MgO contents (<0.5 weight percent) and higher K_2O contents (max 5.5 weight percent) at comparable SiO_2 contents (fig. 5; table 2; Pallister and others, this volume, chap. 30). On the basis of variations in MgO and K_2O contents, glasses can be divided into what appear to be older glassy ash fragments and juvenile material. Judging from these criteria, none of the clean-glass analyses from the October 1 and 5, 2004, explosions are considered juvenile, although glasses with juvenile characteristics were observed in ash from the October 4, 2004, explosion (fig. 5). However, the high crystallinity of the groundmass, resulting in few clean-glass analyses, precludes definitive estimates of the proportion of juvenile glass observed in early eruptive material. In addition, all of the analyzed pumice fragments fall within the compositional fields defining older volcanic deposits (fig. 5).

Backscattered electron images provide a textural comparison between juvenile crystalline groundmass (fig. 10*B*) and a pumiceous glass fragment compositionally similar to older volcanic deposits (fig. 10*D*). Both textural and compositional comparisons between the various groundmass types are critical to avoiding a common misconception that glassy ash particles (for example, fig. 10*D*) are always representative of the juvenile component associated with an eruption, as previously attributed (for example, Sarna-Wojcicki and others, 1981b; Swanson and others, 1995; Watanabe and others, 1999).

Previous studies of 1980s tephra and dome samples indicate that the Li content in feldspar from 1980–85 lavas and tephras is as high as ~25 µg/g (fig. 11; Berlo and others, 2004; Kent and others, this volume, chap. 35). In contrast, the Li content in plagioclase from early 2004 dome sample SH304-2A (erupted approx. Oct. 18, 2004) ranges from 28 to 43 µg/g Li, distinctly higher than that in older Mount St. Helens feldspar (Kent and others, this volume, chap. 35). This difference provides a means to trace the contribution to ash samples collected between October 1 to October 5, 2004, from juvenile magma (figs. 9, 11). As previously discussed, after dome sample SH304-2A was collected, Li contents dropped to levels similar those in 1980–85 materials (<30 µg/g), thus limiting the usefulness of this approach to material produced only at the start of an eruption.

Measured Li contents in plagioclase in ash erupted from October 1, 2004, to March 9, 2005, form two populations. The Li contents of most plagioclase phenocrysts range from 10 to 25 µg/g and appear to be broadly normally distributed around a mean of 19 µg/g (fig. 9), whereas a smaller subset (~25 percent) of grains have distinctly higher Li contents (max 46 µg/g). On a cumulative-probability plot (fig. 11*B*), most plagioclase phenocrysts lie on a straight-line segment, with a mean of ~18 µg/g, consistent with a near-normal distribution; however, a distinct break in slope occurs at ~30 µg/g, suggesting that the higher Li contents may derive from a different population. If we divide the samples into two groups, using a Li content of 30 µg/g as a boundary, application of Student's *t* test (appropriate for comparing the means of small samples that may show some departure from a normal distribution; for example, Borradaile, 2003) suggests that these two sample

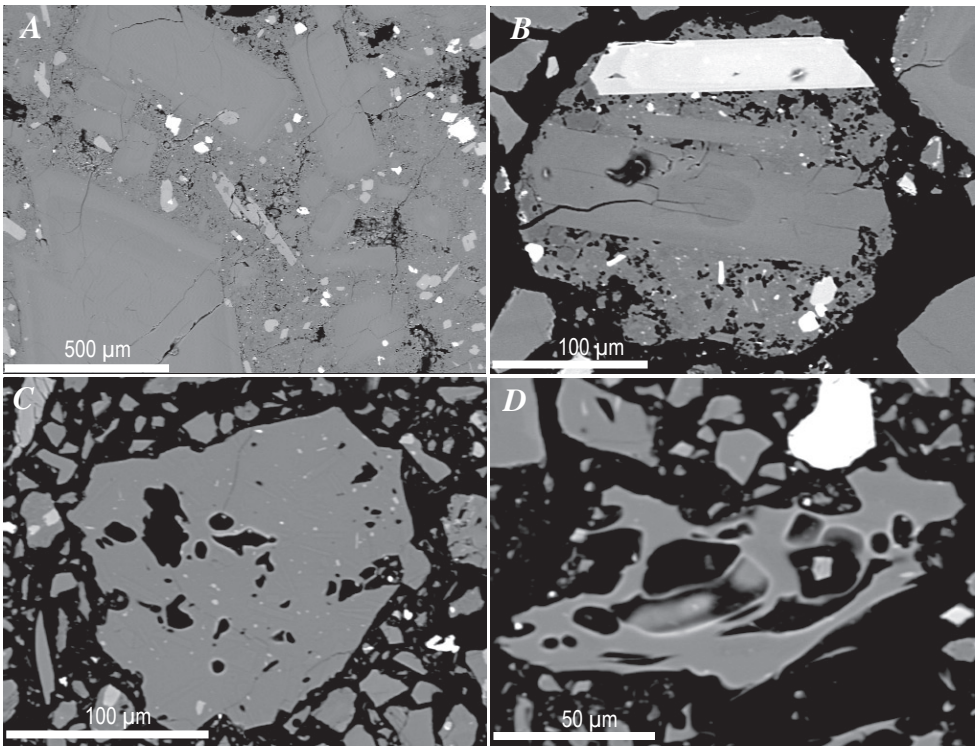

Figure 10. Backscattered electron images of dome rock, ash fragments, and pumice fragments. *A,* Groundmass from dome sample SH304. *B,* Ash fragment from sample MSH04MR_11_4 (feldspar Li content of 33.7 µg/g). *C,* Glassy fragment of ash with extensive plagioclase microlite crystallization from sample MSH04E2A03_A1. *D,* Pumice fragment from sample MSH04E2A03_A1.

groups are significantly different at the >99.9-percent confidence level. Furthermore, the >30-µg/g-Li sample group is indistinguishable from plagioclase from samples SH304-2A and SH304-2C, whereas the <30-µg/g-Li sample group is indistinguishable from plagioclase from the 1981–85 dome samples (table 3). From this we suggest that the plagioclase containing >30 µg/g Li in ash produced by explosions from October 1 to 5, 2004, was derived from Li-enriched juvenile magma similar to that sampled by dome samples SH304-2A and SH304-2C.

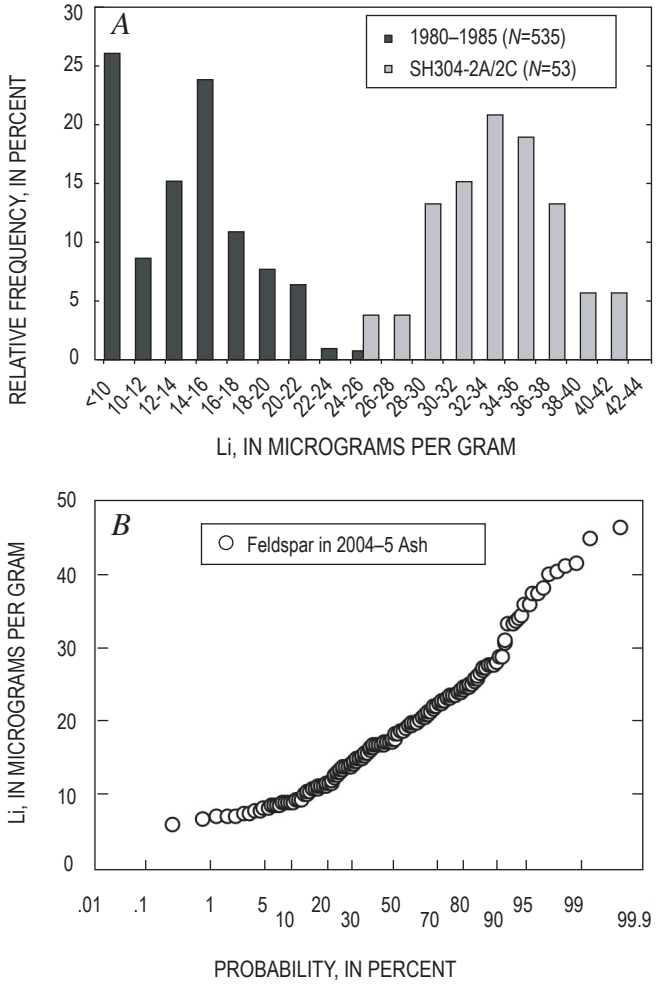

Figure 11. Li contents in feldspar in dome rocks. *A,* Histogram of Li contents in feldspar in 1980–85 dome rocks (black bars, *N*=535) and in sample SH304 (gray bars; *N*=53). Data for 1980–85 samples from Berlo and others (2004) and Kent and others (this volume, chap. 35); data for sample SH304 from Kent and others (this volume, chap. 35). *B,* Li content versus probability for 2004–5 feldspar in ash. In a single normally distributed population, this relation would plot as a straight line. Distinct change in slope at 30 µg/g Li content suggests that multiple populations of plagioclase grains are present in ash samples.

Li enrichment in feldspar, which is interpreted to result from transfer of a magmatic vapor phase, is expected to occur only within juvenile material, not in older conduit material or debris covering the conduit (Kent and others, 2007). This interpretation is supported by (1) the absence of anomalous Li contents in plagioclase in gabbroic inclusions; and (2) the high Li contents (max ~200 µg/g) in amphibole-hosted melt inclusions, consistent with concentrations required in the melt, as estimated from plagioclase/melt partitioning (Bindeman and others, 1998; Kent and others, 2007). On the basis of this evidence, 8 out of 39 (~20 percent) of the feldspars from the October 1 to 5, 2004, ash deposits are juvenile. Though not definitive, the proportion of juvenile material also increases from October 1 to October 4, 2004, suggesting a possible increased involvement of juvenile material in explosions. One explanation for this increase is upward movement of magma within the shallow conduit, consistent with the appearance of hot dacite on the surface of the crater floor on October 11, 2004.

A discrepancy is evident between estimates of the proportion of juvenile material in ash based on Li contents in feldspars versus the compositions of glass fragments. A possible cause for this discrepancy is that only a few clean-glass analyses were obtained as a result of quartz and feldspar microlite crystallization (figs. 4, 10). This same microcrystalline texture is also observed in dome samples, suggesting that the shallow magmatic crystallization observed in dome rocks occurred before fragmentation of the dacite. Because most of the juvenile groundmass had crystallized before eruption, clean-glass analyses ultimately underestimate the proportion of juvenile material in early ash samples.

Evidence for a Volatile Eruption Trigger

The high Li contents measured in early-erupted feldspar from the ash (max 48 µg/g) and dome samples (max 41 µg/g) may indicate an increase in volatile components at the initiation of the 2004 eruption. As previously discussed, the high Li content measured in feldspar would require a Li content in melt of ~200 µg/g, on the basis of plagioclase/melt partition coefficients (Bindeman and others, 1998), despite the lower Li contents (21–28 µg/g) measured in bulk dacite. As suggested by Berlo and others (2004), the Li-rich feldspar could be explained by enrichment of shallow-stored magma through upward movement of an alkali-enriched vapor from deeper within the magmatic system. Because the highest Li contents were measured only before collection of sample SH305-1 (estimated eruption date, Nov. 20, 2004), this difference suggests greater vapor enrichment during the early stages of the eruption. Kent and others (2007) estimate that vapor enrichment must have occurred within the year before the eruption (potentially within just a few days) before the eruption, because earlier enrichment would have resulted in diffusional equilibration of feldspar in gabbroic inclusions—which have lower Li contents than groundmass plagioclase. The decrease in feldspar Li contents over time observed in the dome dacite samples may indicate that the volatile-enriched magma

Table 3. Statistics of Li contents in feldspar in 2004–5 ash, new dome lava, and 1980–85 dome lava.

[2004 sample is SH304-2A, erupted about Oct. 18 and collected Nov. 4, 2004, showing data from Kent and others (this volume, chap. 35). Li contents in feldspar for 1980 materials from Berlo and others (2004). Data for 1981–85 from samples SH100, SH141, and SH187, analyzed at Oregon State University (Kent and others, this volume, chap. 35). Li contents in feldspars from ash produced during the 2004–5 eruption are divided into"Li-poor" (<30 μg/g) and "Li-rich" (>30 μg/g) groups on the basis of statistical analysis (fig. 11; see text for discussion).]

	Feldspar in dome rocks			Feldspar in 2004–5 ash	
	2004	1981–85	1980	Li-poor	Li-rich
Mean	33.4	17.1	13.1	17.6	37.5
Standard deviation (1σ)	3.8	4.3	4.6	5.8	4.5
Number of samples (N)	53	28	507	177	18

was only a shallow cap on a larger magma body (Kent and others, this volume, chap. 35).

A CO_2 output of 2,415 t/d, measured on October 7, 2004, followed by a steady decline in ensuing months also suggests a greater volume of gas early in the eruption, although the higher gas output could also result from higher extrusion rates early in the eruption (Gerlach and others, this volume, chap. 26). Together, both the high Li contents in feldspar and the highest CO_2 output measured on October 7, 2004, may indicate the presence of an excess volatile phase, partly resulting from volatile components transferred from a deeper magma, before the onset of the eruption. An increase in vapor pressure may have helped drive the explosions of October 2004. (For a more detailed discussion on the formation of the vapor phase, see Berlo and others, 2004, and Kent and others, this volume, chap. 35.)

Ash Generation

Airborne ash at Mount St. Helens is produced by both vent explosions and rockfalls or rock avalanches. Two general mechanisms are typically described for the generation of ash during vent explosions. In magmatic explosions, exsolution and expansion of gases in magma during its ascent leads to vesiculation and fragmentation of the magma (Heiken, 1972; Cashman and others, 2000). In contrast, phreatomagmatic eruptions result primarily from the rapid expansion, at Mount St. Helens, of meteoric water as it interacts with magma and (or) hot rock at depth (Morrissey and others, 2000).

Ash from Mount St. Helens' 2004–5 vent explosions is dispersed more widely than ash from rockfalls, with fallout reported as far as Ellensburg, Wash., after the March 8, 2005, vent explosion (Mastin and others, 2005; Scott and others, this volume, chap. 1). Rockfalls and rock avalanches in this eruption resulted from dome growth and oversteepening (Vallance and others, this volume, chap. 9). Rockfalls and rock avalanches, with elutriation of fine ash particles, occur much more frequently than vent explosions and are typically smaller, sending ash as high as 3,000 m into the air before it falls proximal to the edifice (Scott and others, this volume, chap. 1). In addition to vent explosions and rockfalls, small volumes of airborne ash may be distributed by elutriation during steaming of the dome or resuspended off crater walls by strong winds—relatively low energy mechanisms for ash transportation.

Mechanisms of ash generation and distribution of the 2004–5 Mount St. Helens eruption are not easily discernible by using criteria of grain shape, volume of glass, or textural and compositional heterogeneity of ash particles (see above descriptions). In this eruption, very little glassy material was present in the ash, and <5 percent of the clean-glass samples are considered juvenile. Juvenile groundmass observed in the dome and in the ash is mostly crystalline (quartz and feldspar), with localized vesiculation and devitrification (figs. 10*A*, 10*B*). Water-by-difference measurements of melt inclusions in phenocrysts from dome samples SH304 and SH305 support gas emission data which, for this eruption, indicate that juvenile magma had degassed extensively before eruption (Gerlach and others, this volume, chap. 26; Pallister and others, this volume, chap. 30). The degassed and crystallized nature of the magma may have reduced the role of expansion of magmatic volatile components in the generation of ash, during either vent explosions or rockfalls and rock avalanches. In addition, the abundance of lithic fragments and paucity of glass shards or pumice fragments suggest that vent explosions (Oct. 1, 4, and 5, 2004; Jan. 16, 2005; Mar. 8, 2005) are dominantly phreatic in origin and that crystallization of the rising magma had occurred before the explosive events.

By comparing geochemical analyses of feldspar and glass in conjunction with the backscattered electron imaging of ash derived from vent explosions and rockfalls or rock avalanches, we attempted to distinguish between possible causes and mechanisms for the dispersal of ash. Major-element compositions of matrix glass and glass inclusions from the January 13, 2005, rockfall ash correlate well with juvenile compositions determined from glass analyses of dome samples SH304 and SH305 (fig. 5). In contrast, less than half of the glass analy-

ses from the January 16, 2005, vent explosion correlate with juvenile fields. This discrepancy demonstrates that the vent eruptions entrain more of the exotic fragments derived from crater debris in the vent area.

A distinct contrast is observed when comparing glass compositions from the rockfall events of November 4, 2004, and January 13, 2005. Whereas the ash from the November 4, 2004, event is dominated by older glass, the ash from the January 13, 2005, event is dominated by juvenile glass (fig. 5), suggesting that the part of the early dome (or uplift area) responsible for ash generation contained a significant amount of older material but by January 2005 was composed dominantly of juvenile dacitic material. This conclusion is also supported by field observations and pre-November 2004 dome samples (Pallister and others, this volume, chap. 30; Reagan and others, this volume, chap. 37).

Juvenile ash fragments from large rockfalls (Nov. 4, 2004, and Jan. 13, 2005) and vent explosions (Jan. 16, 2005, and Mar. 8, 2005) have nearly identical groundmass textures, as described above (fig. 12). Both processes produce strikingly similar grain shapes. Ash particles dominated by large phenocrysts commonly reflect the general shape of those phenocrysts and are more angular, whereas ash particles dominated by groundmass typically range in shape from subangular to round. In principle, particle shape in magmatic eruptions is controlled by the shape and abundance of vesicles, whereas glassy fragments in phreatomagmatic eruptions are commonly pyramidal or blocky (Heiken, 1972). In both magmatic and phreatomagmatic eruptions, however, relatively rapid cooling should result in the generation of glassy material. In contrast, in an experimental study of dacite fragmentation using Mount St. Helens 1980 gray dacite, similar to the cryptodome with low H_2O contents and composed of ~30 volume percent phenocrysts, the material produced brittle, angular fragments (Alidibirov and Dingwell, 1996). This material more closely resembles some of the particles observed in recent rockfalls and explosions, suggesting

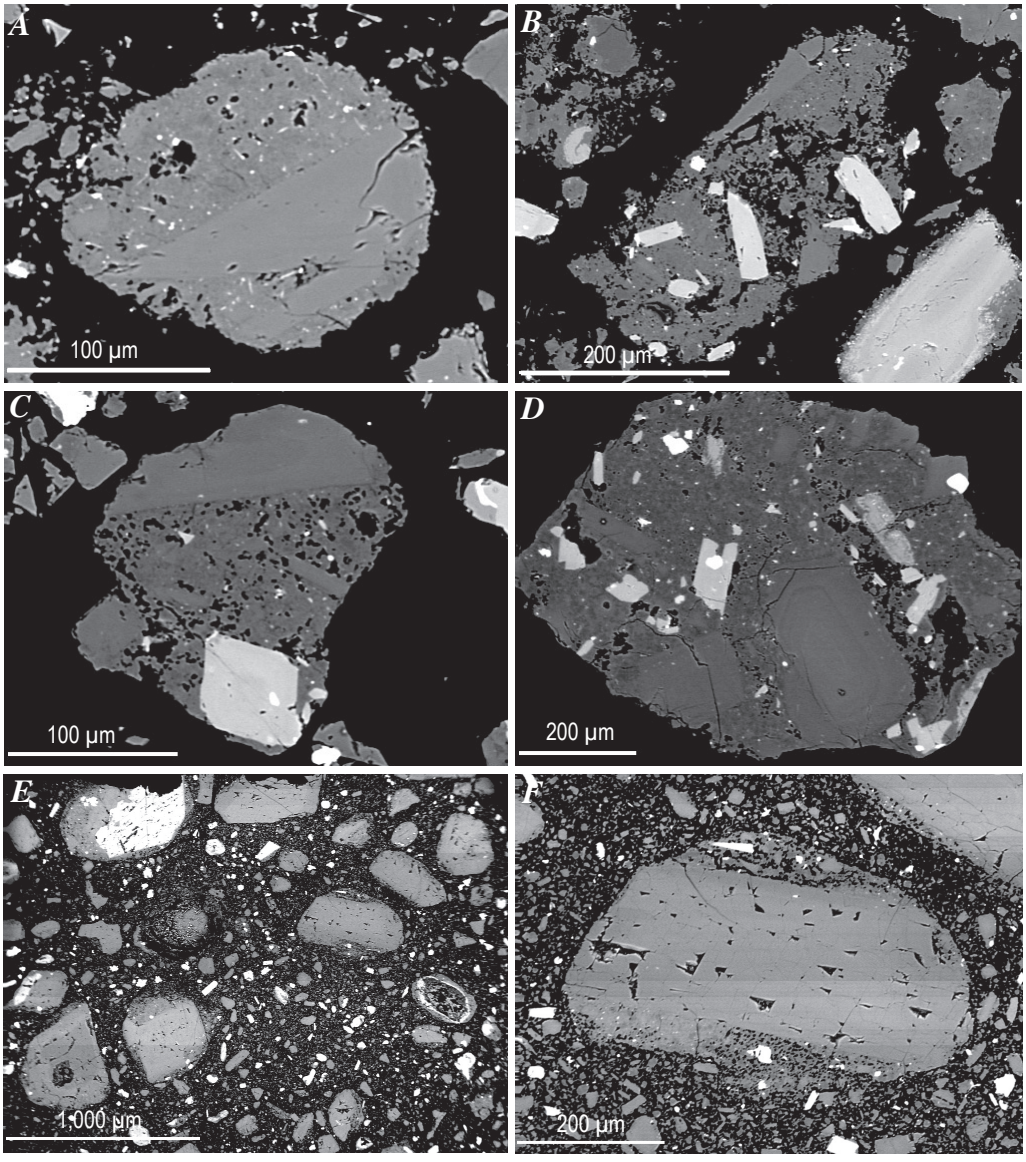

Figure 12. Backscattered electron images of characteristic ash particles from dome rockfalls *(A, B)*, vent explosions *(C, D)* and dome gouge *(E, F)*. *A,* Rounded ash fragment from sample MSH05JP_1_14A, from rockfall on January 13, 2005. *B,* More highly disaggregated ash particle from same sample as in figure 12*A*. *C,* Subrounded ash fragment with grain shape controlled by larger feldspar and hypersthene phenocrysts from sample MSH05JV_1_19, from explosion of January 16, 2005. *D,* Largely devitrified ash particle (see X-ray map in fig. 3) from explosion of March 8, 2005. *E,* Low-magnification image of disaggregated dome gouge from sample SH307-1. *F,* Enlargement of rounded clast in figure 12*E*, showing characteristic ash morphology.

that fragmentation may have occurred by brittle failure without frothing or vesiculation of the magma. Similarities in grain shape and texture of the juvenile matrix from different types of events suggest that the ash is generated by related processes.

The disaggregation of the outer 1 to 3 m of the dome (dome fault gouge; see Cashman and others, this volume, chap. 19, for a detailed description) provides an additional potential source for ash particles, independent of magmatic fragmentation. Gouge particles are dominantly subangular to rounded, similar to the particles observed in a large proportion of the ash (figs. 12*E*, 12*F*). Groundmass textures of dome gouge (sample SH303-1, table 1) extruded on October 18, 2004, are heterogeneous, suggesting that at that time the gouge contained a high percentage of exotic wallrock fragments.

The heterogeneity of the dome gouge may also explain the dominance of glass compositions representative of older eruptive events in the November 4, 2004, dome-collapse ash. In addition, Li contents in feldspar from the November 4, 2004, ash closely resemble those of the gouge, which are dominantly low (<30 µg/g) and do not correlate well with those of either dome samples SH304 or SH305 (figs. 9, 11; Kent and others, this volume, chap. 35). Recall that feldspars with Li contents below 30 µg/g are a statistically distinct group from the Li-rich population and correlate with older Mount St. Helens eruptive products (fig. 11). In contrast, the January 13, 2005, dome-collapse ash is significantly more homogenous, with glass compositions matching that of the growing dome (fig. 5). This homogeneity was also observed in the dome fault gouge (sample SH307-1, table 1) collected on February 22, 2005, with groundmass textures resembling those of the growing dome, and groundmass textures and grain shapes similar to those observed in the ash.

Textural and geochemical evidence presented here suggests that airborne ash in the 2004–6 eruption is largely generated from the dome fault gouge. Large dome-collapse events and explosions may also produce a significant component of material resulting from brittle failure of the dacite during expansion of volatile components, despite low volatile contents. These particles would have groundmass textures similar to dome gouge but would likely have angular to subangular grain shapes instead of the more rounded particles found within the gouge (Alidibirov and Dingwell, 1996; Cashman and others, this volume, chap. 19).

The particle size distributions of ash samples generated from both dome collapse and vent explosions overlap significantly, largely owing to the distance to the vent at which samples were collected; therefore, particle size is inconclusive for distinguishing source mechanism (fig. 13). Mean particle size varies but generally decreases with increasing distance from the vent. In addition, the mean particle size of ash from vent explosions is significantly greater than that from dome-collapse events, despite collection farther from the vent, illustrating the farther transport of coarse ash during more explosive events. The particle size distribution of dome gouge differs from that of ash deposited from either dome-collapse events or vent explosions (fig. 13). However, because variables resulting in mechanical sorting of the ash, including explosivity of the eruption, windspeed, height of the ash cloud, and distance to the vent, are not taken into account in this comparison, particle size distributions cannot be used to corroborate textural evidence which suggests that a large proportion of the ash is derived from the dome fault gouge.

Distal ash believed to remobilize during steaming or from strong winds is dissimilar to ash from the rockfalls and vent explosions. The ash collected between October 6 and November 2, 2004, contains abundant exotic particles and pumice fragments and substantially less of the highly crystalline groundmass characteristic of the juvenile dome material commonly erupted during discrete ash-producing events. Only a small proportion of clean juvenile glass is present in all of the ash samples collected during this interval, and no systematic variation is observed in the proportion of juvenile glass over time, despite the appearance of hot dacite on October 11, 2004. Similar results are observed for Li contents in feldspar during this period, with high Li contents in only ~4 percent (3 of 79) of analyzed feldspar, despite identifying ~22 percent (5 of 23) of juvenile feldspar in the fine material in the sample collected from the October 20, 2004, crater debris flow (sample SH300-1, table 1). Remobilization of ash particles from the crater walls by strong winds, and elutriation of fine ash particles from rising steam, appear to have (1) preferentially transported low-density material, such as pumice fragments; and (2) resulted in apparent dilution of the estimated proportion of juvenile material as a result of greater contamination from older volcanic rocks. Despite the continuous ash collection, therefore, sampling of discrete events appears to provide a more representative depiction of current eruptive conditions.

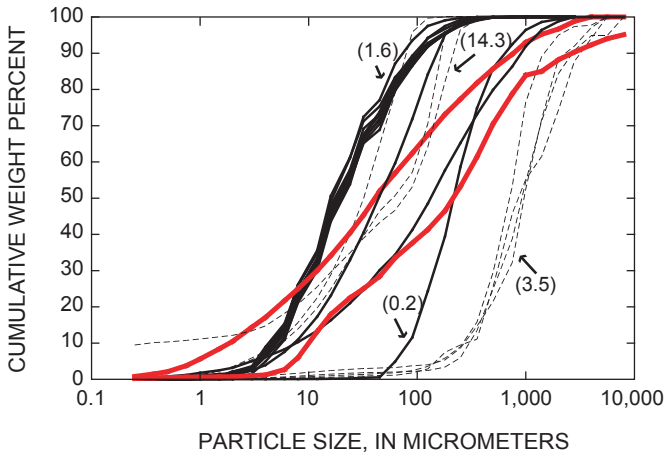

Figure 13. Particle size distribution for ash derived from rockfalls and rock avalanches (black solid lines, *N*=13), vent explosions (dashed lines, *N*=7), and dome gouge (red solid lines, *N*=2). Wide variation is partly attributable to varying distance from vent (numbers in parentheses are distance in kilometers to vent) and explosivity of eruption. Note that even at greater distance from vent, explosive deposits generally have a larger average particle size.

Conclusions

This textural and geochemical examination of 2004–5 Mount St. Helens ash provides several important observations and conclusions with regard to early eruptive events and processes of ash generation and transportation.

1. The Li content in feldspar from dome sample SH304 is >30 µg/g, significantly higher than in older Mount St. Helens eruptive material, allowing for the identification of juvenile plagioclase in the ash. Li contents may indicate an increase in the proportion of juvenile material from October 1 through 4, 2004. High Li contents in feldspar are useful as a tracer for juvenile material only during the beginning stages of the eruption—within 6 weeks after eruptive onset—because after about November 20, 2004 (estimated eruption date of sample SH305), Li contents in feldspar dropped to levels similar to that observed during the period 1980–86. The decrease in Li content also suggests that the volatile-enriched magma was only a shallow cap on a larger magma body.

2. The clean glass in ash samples is mostly older volcanic material. Juvenile groundmass is typically crystalline (quartz and feldspar), with localized devitrification and patchy, very fine vesiculation, contrary to the traditional assumption that clean glass is juvenile volcanic material. Estimates of the proportion of juvenile material based on glass analyses are significantly lower than those based on Li content in plagioclase.

3. Groundmass textures, grain shapes, and compositional similarities among ash from vent explosions, rockfalls, and dome fault gouge particles suggest that the gouge is a significant source of ash material. Despite differences in particle size, the grain shapes and textures of particles from rockfalls and vent explosions are relatively similar, suggesting that the ash is derived by a similar mechanism in both events. The heterogeneity observed in early ash samples correlates with observations that the early extruded dome material and fault gouge contained a significant proportion of older volcanic material. The increase in the homogeneity of ash over time is consistent with a similar trend in dome and fault gouge samples.

4. The presence of an excess volatile phase, as indicated by the high Li contents in feldspar, may indicate the presence of a greater proportion of vapor at the top of the conduit where shallow-stored magmas had stalled. This excess vapor may have been the catalyst for initiation of the 2004–6 eruption.

5. Continuous monitoring of ash samples during periods of relatively low eruptive activity may not provide a representative depiction of the current eruptive processes, owing to contamination from other debris. Therefore, collection and monitoring of discrete dome-collapse events and vent explosions provides the most accurate record of the current eruption.

Acknowledgments

We thank all of the Cascades Volcano Observatory staff and volunteers who assisted in the collection of Mount St. Helens ash, especially S. McConnell, T. Herriott, and A. Eckberg, who assisted with drying, sorting, and weighing of ash samples, and D. Gooding and D. Ramsey for assistance in the field and with the collection site mapping. Electron microprobe time at Oregon State University was provided by F. Tepley. LA-ICP-MS analyses were performed at the W.M. Keck Collaboratory for Plasma Spectrometry, Oregon State University. Detailed reviews by J. Larsen and R. Hoblitt greatly improved the manuscript. The Mount St. Helens petrology working group provided valuable discussion and feedback for this study. This research was supported in part by National Science Foundation grant EAR 0440382.

References Cited

Alidibirov, M., and Dingwell, D.B., 1996, Magma fragmentation by rapid decompression: Nature, v. 380, no. 6570, p. 146–148, doi:10.1038/380146a0.

Berlo, K., Blundy, J., Turner, S., Cashman, K., Hawkesworth, C., and Black, S., 2004, Geochemical precursors to volcanic activity at Mount St. Helens, USA: Science, v. 306, p. 1167–1169.

Bindeman, I.N., Davis, A.M., and Drake, M.J., 1998, Ion microprobe study of plagioclase-basalt partition experiments at natural concentration levels of trace elements: Geochimica et Cosmochimica Acta, v. 62, p. 1175–1193.

Borradaile, G., 2003, Statistics of Earth Science data; their distribution in time, space, and orientation: New York, Springer, 351 p.

Cashman, K.V., and Hoblitt, R.P., 2004, Magmatic precursors to the 18 May 1980 eruption of Mount St. Helens, USA: Geology, v. 32, no. 2, p. 141–144, doi:10.1130/G20078.1.

Cashman, K.V., Sturtevant, B., Papale, P., and Navon, O., 2000, Magmatic fragmentation, *in* Sigurdsson, H., ed., Encyclopedia of volcanoes: London, Academic Press, p. 421–430.

Cashman, K.V., Thornber, C.R., and Pallister, J.S., 2008, From dome to dust; shallow crystallization and fragmentation of conduit magma during the 2004–2006 dome extrusion of Mount St. Helens, Washington, chap. 19 *of* Sherrod, D.R., Scott, W.E., and Stauffer, P.H., eds., A volcano rekindled; the renewed eruption of Mount St. Helens, 2004–2006: U.S. Geological Survey Professional Paper 1750 (this volume).

Friedman, J.D., Olhoeft, G.R., Johnson, G.R., and Frank, D., 1981, Heat content and thermal energy of the June dacite

dome in relation to total energy yield, May–October 1980, *in* Lipman, P.W., and Mullineaux, D.R., eds., The 1980 eruptions of Mount St. Helens, Washington: U.S. Geological Survey Professional Paper 1250, p. 557–567.

Gerlach, T.M., McGee, K.A., and Doukas, M.P., 2008, Emission rates of CO_2, SO_2, and H_2S, scrubbing, and preeruption excess volatiles at Mount St. Helens, 2004–2005, chap. 26 *of* Sherrod, D.R., Scott, W.E., and Stauffer, P.H., eds., A volcano rekindled; the renewed eruption of Mount St. Helens, 2004–2006: U.S. Geological Survey Professional Paper 1750 (this volume).

Heiken, G., 1972, Morphology and petrography of volcanic ashes: Geological Society of America Bulletin, v. 83, no. 7, p. 1961–1987.

Houghton, B.F., Wilson, C.J.N., Smith, R.T., and Gilbert, J.S., 2000, Phreatoplinian eruptions, *in* Sigurdsson, H., ed., Encyclopedia of volcanoes: London, Academic Press, p. 513–525.

Kent, A.J.R., Blundy, J., Cashman, K.V., Cooper, K.M., Donnelly, C., Pallister, J.S., Reagan, M., Rowe, M.C., and Thornber, C.R., 2007, Vapor transfer prior to the October 2004 eruption of Mount St. Helens, Washington: Geology, v. 35, no. 3, p. 231–234, doi:10.1130/G22809A.1.

Kent, A.J.R., Rowe, M.C., Thornber, C.R., and Pallister, J.S., 2008, Trace element and Pb isotope composition of plagioclase from dome samples from the 2004–2005 eruption of Mount St Helens, Washington, chap. 35 *of* Sherrod, D.R., Scott, W.E., and Stauffer, P.H., eds., A volcano rekindled; the renewed eruption of Mount St. Helens, 2004–2006: U.S. Geological Survey Professional Paper 1750 (this volume).

LaHusen, R.G., Swinford, K.J., Logan, M., and Lisowski, M., 2008, Instrumentation in remote and dangerous settings; examples using data from GPS "spider" deployments during the 2004–2005 eruption of Mount St. Helens, Washington, chap. 16 *of* Sherrod, D.R., Scott, W.E., and Stauffer, P.H., eds., A volcano rekindled; the renewed eruption of Mount St. Helens, 2004–2006: U.S. Geological Survey Professional Paper 1750 (this volume).

Major, J.J., Scott, W.E., Driedger, C., and Dzurisin, D., 2005, Mount St. Helens erupts again; activity from September 2004 through March 2005: U.S. Geological Survey Fact Sheet 2005–3036, 4 p.

Mastin, L.G., Sherrod, D.R., Vallance, J.W., Thornber, C.R., and Ewert, J.W., 2005, The roles of magmatic and external water in the March 8 tephra eruption at Mount St. Helens as assessed by a 1-D steady plume-height model [abs.]: Eos (American Geophysical Union Transactions), v. 86, no. 52, Fall Meeting Supplement, Abs. V53D-1597.

Melson, W.G., 1983, Monitoring the 1980–1982 eruptions of Mount St. Helens; compositions and abundances of glass: Science, v. 221, no. 4618, p. 1387–1391.

Morgan, G.B., IV, and London, D., 1996, Optimizing the electron microprobe analysis of hydrous alkali aluminosilicate glasses: American Mineralogist, v. 81, 1176–1185.

Morrissey, M., Zimanowski, B., Wohletz, K., and Buettner, R., 2000, Phreatomagmatic fragmentation, *in* Sigurdsson, H., ed., Encyclopedia of volcanoes: London, Academic Press, p. 431–445.

Pallister, J.S., Hoblitt, R.P., and Reyes, A.G, 1992, A basalt trigger for the 1991 eruptions of Pinatubo volcano?: Nature, v. 356, p. 426–428.

Pallister, J.S., Thornber, C.R., Cashman, K.V., Clynne, M.A., Lowers, H.A., Mandeville, C.W., Brownfield, I.K., and Meeker, G.P., 2008, Petrology of the 2004–2006 Mount St. Helens lava dome—implications for magmatic plumbing and eruption triggering, chap. 30 *of* Sherrod, D.R., Scott, W.E., and Stauffer, P.H., eds., A volcano rekindled; the renewed eruption of Mount St. Helens, 2004–2006: U.S. Geological Survey Professional Paper 1750 (this volume).

Reagan, M.K., Cooper, K.M., Pallister, J.S., Thornber, C.R., and Wortel, M., 2008, Timing of degassing and plagioclase growth in lavas erupted from Mount St. Helens, 2004–2005, from ^{210}Po-^{210}Pb-^{226}Ra disequilibria, chap. 37 *of* Sherrod, D.R., Scott, W.E., and Stauffer, P.H., eds., A volcano rekindled; the renewed eruption of Mount St. Helens, 2004–2006: U.S. Geological Survey Professional Paper 1750 (this volume).

Rowe, M.C., Thornber, C., and Kent, A.J.R., 2005, Petrology and geochemistry of Mount St. Helens ash before and during continuous dome extrusion [abs.]: Geochimica et Cosmochimica Acta, v. 69, no. 10, supp. 1, p. A272.

Rowe, M.C., Thornber, C.R., Gooding, D.J., and Pallister, J.S., 2008, Catalog of Mount St. Helens 2004–2005 tephra samples with major- and trace-element geochemistry: U.S. Geological Survey Open-File Report 2008–1131, 7 p, with digital database.

Rutherford, M.J., and Devine, J.D., III, 2008, Magmatic conditions and processes in the storage zone of the 2004–2006 Mount St. Helens dacite, chap. 31 *of* Sherrod, D.R., Scott, W.E., and Stauffer, P.H., eds., A volcano rekindled; the renewed eruption of Mount St. Helens, 2004–2006: U.S. Geological Survey Professional Paper 1750 (this volume).

Rutherford, M.J., and Hill, P.M., 1993, Magma ascent rates from amphibole breakdown; an experimental study applied to the 1980–1986 Mount St. Helens eruptions: Journal of Geophysical Research, v. 98, no. B11, p. 19667–19685.

Sarna-Wojcicki, A.M., Meyer, C.E., Woodward, M.J., and Lamothe, P.J., 1981a, Composition of air-fall ash erupted on May 18, May 25, June 12, July 22, and August 7, *in* Lip-

man, P.W., and Mullineaux, D.R., eds., The 1980 eruptions of Mount St. Helens, Washington: U.S. Geological Survey Professional Paper 1250, p. 667–681.

Sarna-Wojcicki, A.M., Waitt, R.B., Jr., Woodward, M.J., Shipley, S., and Rivera, J., 1981b, Premagmatic ash erupted from March 27 through May 14, 1980—extent, mass, volume, and composition, *in* Lipman, P.W., and Mullineaux, D.R., eds., The 1980 eruptions of Mount St. Helens, Washington: U.S. Geological Survey Professional Paper 1250, p. 569–575.

Schiavi, F., Tiepolo, M., Pompilio, M., and Vannucci, R., 2006, Tracking magma dynamics by laser ablation (LA)-ICPMS trace element analysis of glass in volcanic ash: the 1995 activity of Mt. Etna: Geophysical Research Letters, v. 33, L05304, 4p., doi:10.1029/2005GL024789.

Scott, W.E., Sherrod, D.R., and Gardner, C.A., 2008, Overview of the 2004 to 2006, and continuing, eruption of Mount St. Helens, Washington, chap. 1 *of* Sherrod, D.R., Scott, W.E., and Stauffer, P.H., eds., A volcano rekindled; the renewed eruption of Mount St. Helens, 2004–2006: U.S. Geological Survey Professional Paper 1750 (this volume).

Sparks, R.S.J., Bursik, M.I., Carey, S.N., Gilbert, J.S., Glaze, L.S., Sigurdsson, H., and Woods, A.W., 1997, Volcanic plumes: New York, John Wiley, 574 p.

Streck, M.J., Broderick, C.A., Thornber, C.R., Clynne, M.A., and Pallister, J.S., 2008, Plagioclase populations and zoning in dacite of the 2004–2005 Mount St. Helens eruption; constraints for magma origin and dynamics, chap. 34 *of* Sherrod, D.R., Scott, W.E., and Stauffer, P.H., eds., A volcano rekindled; the renewed eruption of Mount St. Helens, 2004–2006: U.S. Geological Survey Professional Paper 1750 (this volume).

Swanson, S.E., Nye, C.J., Miller, T.P., and Avery, V.F., 1994, Geochemistry of the 1989–1990 eruption of Redoubt Volcano; part II, mineral and glass chemistry: Journal of Volcanology and Geothermal Research, v. 62, nos. 1–4, p. 453–468.

Swanson, S.E., Harbin, M.L., and Riehle, J.R., 1995, Use of volcanic glass from ash as a monitoring tool; an example from the 1992 eruptions of Crater Peak, Mount Spurr volcano, Alaska, *in* Keith, T.E.C., ed., The 1992 eruptions of Crater Peak vent, Mount Spurr volcano, Alaska: U.S. Geological Survey Bulletin 2139, p. 129–137.

Taddeucci, J., Pompilio, M., and Scarlato, P., 2002, Monitoring the explosive activity of the July–August 2001 eruption of Mt. Etna (Italy) by ash characterization: Geophysical Research Letters, v. 29, no. 8, 1230, 4 p., doi:10.1029/2001GL014372.

Thomas, E., Varekamp, J.C., and Busheck P.R., 1982, Zinc enrichment in the phreatic ashes of Mt. St. Helens, April 1980: Journal of Volcanology and Geothermal Research, v. 12, nos. 3–4, p. 339–350.

Thornber, C.R., Pallister, J.S., Lowers, H.A., Rowe, M.C., Mandeville, C.W., and Meeker, G.P., 2008a, Chemistry, mineralogy, and petrology of amphibole in Mount St. Helens 2004–2006 dacite, chap. 32 *of* Sherrod, D.R., Scott, W.E., and Stauffer, P.H., eds., A volcano rekindled; the renewed eruption of Mount St. Helens, 2004–2006: U.S. Geological Survey Professional Paper 1750 (this volume).

Thornber, C.R., Pallister, J.S., Rowe, M.C., McConnell, S., Herriott, T.M., Eckberg, A., Stokes, W.C., Johnson Cornelius, D., Conrey, R.M., Hannah, T., Taggart, J.E., Jr., Adams, M., Lamothe, P.J., Budahn, J.R., and Knaack, C.M., 2008b, Catalog of Mount St. Helens 2004–2007 dome samples with major- and trace-element chemistry: U.S. Geological Survey Open-File Report 2008–1130, 9 p., with digital database.

Vallance, J.W., Schneider, D.J., and Schilling, S.P., 2008, Growth of the 2004–2006 lava-dome complex at Mount St. Helens, Washington, chap. 9 *of* Sherrod, D.R., Scott, W.E., and Stauffer, P.H., eds., A volcano rekindled; the renewed eruption of Mount St. Helens, 2004–2006: U.S. Geological Survey Professional Paper 1750 (this volume).

Watanabe, K., Danhara, T., Watanabe, K., Terai, K., and Yamashita, T., 1999, Juvenile volcanic glass erupted before the appearance of the 1991 lava dome, Unzen volcano, Kyushu, Japan: Journal of Volcanology and Geothermal Research, v. 89, p. 113–121.